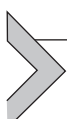


# Remote sensing techniques for estimating evaporation

**Thomas R.H. Holmes**

Hydrological Science Lab, NASA Goddard Space Flight Center, Greenbelt, MD, United States



## 5.1 Introduction

In most general terms, evaporation is the process by which a substance is transformed from its liquid state into vapor. To a hydrologist, evaporation ( $E$ ) refers specifically to the volume of water that evaporates in a given time-period from the Earth's surface into the atmosphere. Evaporation of water completes the hydrological cycle for  $\sim 60\%$  of the precipitation that falls on the land areas of the Earth (e.g., [Oki and Kanae, 2006](#)). This exchange of water vapor between surface and atmosphere is associated with a large transfer of energy in the form of *latent heat*, the conversion of thermal energy into the molecular formation of water vapor from liquid. Latent energy is the dominant source of atmospheric heating when it is liberated through *condensation*. The process of evaporation and condensation transfers more than half of the annual solar energy received by the Earth's land masses to the atmosphere. Evaporation also accompanies the exchange of carbon dioxide and oxygen between growing vegetation and the atmosphere.

Despite this central role for evaporation as a link between the energy, water, and carbon cycles it is one of the least constrained components of the hydrological cycle in land surface models (LSM). Evaporation is difficult to measure remotely because it lacks a direct electromagnetic fingerprint that can be exploited by satellite retrievals. Even if the bulk portion of available energy that is diverted to latent heat can be estimated as a residual of the surface energy balance, the attribution to its source water reservoirs often depends on physical model assumptions. In order to improve estimates of overall evaporation and gain process understanding of the coupled carbon and water cycle, it is important to accurately

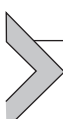
estimate the partitioning of the bulk water flux into soil and vegetation source components. This is because the immediate source of liquid water that evaporates into the atmosphere determines the relative importance of meteorological, biophysiological, and hydrological controls on evaporation. The pathway of the water molecule also affects the circulation rate of the hydrological cycle, with implications for the prediction of available renewable freshwater resources ([Oki and Kanae, 2006](#)).

Passive sources of water for evaporation respond predominantly to meteorological conditions in proportion with water availability and surface texture. There is no biological control on these processes. If the immediate source is the moisture in the soil it is called *soil evaporation*. Globally this constitutes 20%–40% of the total evaporation. Similar to this is evaporation from open water bodies like lakes, rivers, but also temporary pools of rainwater, snow, and ice. A special case of a temporary source of water are pools or drops of water in the canopy that develop when rainwater is intercepted by the leaves. When this water evaporates before it reaches the soil it is referred to as *evaporation of intercepted water* (or interception for short) and can account for 10%–35% of the incident precipitation in forests ([Miralles et al., 2011](#)). Finally, some rainwater (or water from sprinkler irrigation ([Cavero et al., 2009](#)) evaporates before it reaches the ground, but this source of latent heat is typically neglected in land surface models.

In contrast to these passive sources of water for evaporation, the water contained in vegetation tissue is subject to biophysical regulation which can act to moderate the influence of evaporative demand. Plants are also connected to a larger soil reservoir through the root network which may sustain the water supply through periods of drought. When leaf-water evaporates it is called *transpiration* (T), which reflects its role as the main leaf-cooling process and can affect regional temperatures (e.g., [Mueller et al., 2016](#)). Transpiration is the dominant pathway for the total *Evapotranspiration* (ET) and is estimated to account for two-thirds of global land ET based on flux tower measurements ([Jasechko et al., 2013](#); [Schlesinger and Jasechko, 2014](#)). While transpiration helps to keep plants cool, it is also a necessary side-effect of the plants need to breath in CO<sub>2</sub> for photosynthesis and sustain their growth. The biomass yield per unit of water use (crop-per-drop) is an important indicator of agricultural efficiency in water limited regions. Estimating crop water requirements and comparing it to antecedent precipitation is also a straightforward way to assess irrigation requirements ([Allen et al., 1998](#)). If the rate of water loss

cannot be matched by water uptake from the roots, the leaf water potential drops, and ultimately the leaves will wilt. Different species of plants may have different strategies for optimizing their carbon gain while limiting the associated water loss through transpiration and this complicates the modeling of ecosystem response to drought (Konings and Gentine, 2017; Konings et al., 2017). Combined with a longer-term (climatological) baseline, remote sensing estimates of ET are used for (agricultural) drought monitoring (Anderson et al., 2007; Otkin et al., 2016).

Techniques for direct measurement of evaporation include the eddy-covariance (EC) method, Bowen ratio energy balance, and measurement of water loss with lysimeters or mass-balance methods, see for example, Allen et al. (2011) for details. Gas exchange measurements through the EC flux system is now a standard component of the experimental set-up of flux towers, many of which are organized in a global network that includes over 200 towers (Fluxnet; Baldocchi et al., 2001). EC systems have also been mounted on aircraft to measure gas exchange in the boundary layer over larger areal domains (e.g., Anderson et al., 2008; Wolfe et al., 2018). These in situ measurements are invaluable for the development and validation of process descriptions due to their continuous diurnal sampling and wealth of collocated instrumentation. However, to achieve regular monitoring of areal evaporation over land these sparse tower and aircraft measurements need to be combined with sustained satellite remote sensing. This chapter gives a broad overview of the satellite data products (Section 5.2) and the types of observation-based methodologies (Section 5.3) employed in the remote estimation of terrestrial evaporation at diverse spatial domains. Two specific examples of contrasting remote-sensing strategies for estimating evaporation over land are detailed in Sections 5.3.1 and 5.3.2. A brief discussion of more recent developments is included in Section 5.4.



## 5.2 Satellite measurements for evaporation retrievals

There is no single frequency-band that gives a unique fingerprint of evaporation of water into the atmosphere. Remote-sensing approaches for estimating evaporation from space typically rely on an assortment of more readily measurable meteorological and biophysical variables. This makes

remote-sensing of evaporation reliant on several unique parts of the electromagnetic spectrum, from the visible, through infrared and microwave parts of the spectrum.

Many aspects of the vegetation state can be deduced from specific spectral features in the visible to shortwave infrared part of the spectrum. Such information is traditionally summarized in vegetation indices (VI) like leaf area index (LAI, see also Chapter 1.6 for further details) and normalized difference vegetation index (NDVI), and used for land classification. Simple relationships have been developed to estimate areal vegetation fraction from LAI ([Carlson and Ripley, 1997](#)). VI in combination with precipitation and air temperature has some explanatory information on monthly ET measurements. This was utilized by [Jung et al. \(2010\)](#) who trained a machine learning method on global flux tower observations of ET (Fluxnet) to predict global (monthly) land evaporation for 1982–2008 from satellite records of NDVI. Meteorological information like cloud properties and the resulting shortwave and longwave radiative budget of the land surface are dependent on measurements in the visible to infrared parts of the spectrum (e.g., CERES). Several authors have demonstrated the ability to retrieve more detailed plant functional traits and biophysical parameters from the spectral reflectance (e.g., [Serbin et al., 2014](#); [Frankenberg et al., 2011](#)), but these have not yet been incorporated in global ET measurement approaches.

The microwave part of the spectrum has wavelengths of 1 mm to 1 m. These longer waves can penetrate soil, vegetation, and clouds to varying degrees depending on exact wavelength. Microwaves convey information on water content and temperature from the intervening soil, vegetation, and atmospheric layers. Since 1979, space-based passive-microwave (PMW) radiometers measure the emitted radiative energy at frequencies chosen for a variety of remote sensing applications. Their low spatial resolution (10–40 km) is appropriate for continental or global approaches. Radars are used to measure the microwave reflectance at somewhat higher resolution and are important for precipitation measurement ([Smith et al., 2007](#); [Skofronick-Jackson et al., 2017](#)), and surface humidity ([Jackson et al., 2009](#); [Tomita et al., 2018](#)). PMW land surface measurements with particular relevance to ET estimation are long-term soil moisture records (e.g., [Dorigo et al., 2017](#)). PMW observations also convey information on vegetation optical depth ([Owe et al., 2008](#)) which can be used to estimate vegetation water content or biomass

(Liu et al., 2013; Momen et al., 2017), and land surface temperature (LST) (Prigent et al., 2016; Holmes et al., 2016).

The most important part of the spectrum for the remote measurement of ET is the thermal infrared (TIR) region from 1 to 16  $\mu\text{m}$ . Because the phase change of water from liquid to gas represents such a large sink in the surface energy balance, the thermal fingerprint is the most direct diagnostic of latent heat available to remote sensing. This is exploited by surface energy balance approaches (see below) that can leverage the high spatial resolution of TIR-based land surface temperature (LST). Satellites provide thermal radiance with spatial resolutions down to 30 m from low Earth orbit (e.g., Landsat-8 with a bi-weekly revisit time). More moderate spatial resolution but almost daily sampling is afforded by large-swath imagers like VIIRS (375 m) and MODIS (1 km). Multiband thermal infrared radiometers are also available from satellites in geostationary orbit, resulting in diurnal sampling at lower spatial resolution, e.g., 5-minute temporal and 4-km spatial sampling for the GOES Advanced Baseline Imager (ABI), and MSG-SEVIRI (3 km, 15 minutes). The accuracy of the LST retrieval depends on the ability to simultaneously estimate spectral emissivity, which depends on the number of thermal bands. Clouds are almost completely opaque to TIR emission which prevents the retrieval of TIR-based LST from cloud-covered surfaces. It can also impact the analysis of surrounding clear-sky surfaces if clouds are not adequately screened. The efficacy of the cloud screening is an important factor in the precision of LST product and is aided by additional thermal channels.



### 5.3 Evaporation retrieval approaches

ET retrieval approaches combine observable drivers within statistical or process-based methodologies. These process descriptions make use of the concept of *potential evaporation* ( $Ep$ ), which is the rate of evaporation that a large area with growing vegetation would sustain if there is no limit on water availability. It is used in models to represent the atmospheric demand for water, and depends on meteorological conditions like surface humidity, net radiation, wind speed, and near-surface temperature gradients. Only in humid areas does the *actual evaporation* approach (or surpass) the potential for a large part of the year. The challenge is in estimating

the actual evaporation from space, because it also depends on the surface hydrology and biophysical state of the surface.

There are two main categories of satellite-based methodologies to estimate the actual evaporation of water from the land surface. The first category includes methods that combine top-down  $Ep$  estimates with a bottom-up estimate of *evaporative stress*, or reduction from evaporative demand, that is, based on statistical parameterizations and observation-informed surface states. The second category of methodologies takes an entirely top-down approach and solves for actual evaporation as a residual of the surface energy-balance (EB). Although  $Ep$  is used to give context to the estimated  $E$ , it is not a driving dataset in energy-balance solutions.

There are several approaches to parameterize  $Ep$  and evaporative stress that have been adapted to available satellite data sets. The first set of algorithms implements the Penman-Monteith (P-M) formulation ([Monteith, 1965](#)) (e.g., [Cleugh et al., 2007](#); [Mu et al., 2011](#)). The P-M formulation accounts for energy limitations, aerodynamic resistance, and stomatal conductance in its estimate of  $Ep$ , and parameterizes surface resistance based on VIs and surface humidity. The meteorological input requirements can be demanding for global implementation. The [Priestley and Taylor \(1972\)](#) (P-T) formulation is derived from the Penman-Monteith equations for a scenario with plentiful water so that the stomatal resistance is zero. P-T estimates of  $Ep$  are only based on insolation and temperature, which makes them more readily applicable to satellite measurements than the P-M methods. P-T applications must be combined with a way to estimate the reduction from the potential evaporation rate to account for hydrological or biophysical restrictions in water availability. [Fisher et al. \(2008\)](#) used estimates of water vapor pressure to parameterize water availability for soil evaporation, and VIs and air temperature to parameterize vegetation stress. This approach made use of the long satellite record of NDVI and net radiation to produce monthly ET estimates from 1984 to 2006 (PT-JPL). Another distinct approach to estimate evaporative stress is to combine P-T with a running-water-balance with inputs of precipitation and assimilation of soil moisture measurements ([Miralles et al., 2011](#); [Martens et al., 2017](#)). The evaporative stress is subsequently parameterized based on prognostic model states, similar to methods employed by land surface models but with a more direct use of land surface remote sensing, see detailed description below ([Section 5.3.1](#)).

In contrast to these bottom-up approaches to estimating evaporative stress, energy balance approaches estimate actual evaporation directly from

the thermal fingerprint of the latent heat flux. This is the reason that EB approaches are regarded as more purely diagnostic in comparison to approaches that include prognostic information. EB approaches have a long legacy and have found wide application in agricultural studies that benefit from the high spatial resolution afforded by TIR-based imagers. All EB approaches solve for E as the residual of the surface energy balance (net radiation—ground heat flux—sensible heat flux). The first group of larger scale EB approaches treat evaporation as a single bulk flux that includes soil and vegetation sources, for example, SEBAL ([Bastiaanssen et al., 1998](#)), SEBS ([Su, 2002](#)), METRIC ([Allen et al., 2007](#)), and SSEB ([Senay et al., 2016](#)). They evaluate the energy balance at “dry” and “wet” extremes and estimate ET between these extremes based on the spatial variation of internally calibrated temperature within the scene of the satellite image. These EB implementations rely on accurate estimation of the temperature difference between surface and air for the estimation of sensible heat. This is challenging to apply to larger domains due to the inherent biases in the independent estimation of air and surface temperatures.

Two-source EB approaches consider soil and vegetation as separate “sources” for heat and water exchange. They partition LST and net radiation between soil and canopy components and use these to solve a set of physical equations that represent the turbulent flux exchanges between the soil, canopy, and atmosphere ([Kustas and Norman, 1999](#); [Norman et al., 1995](#)). These early applications face the same challenge in estimating consistent surface and air temperatures over large areas as the one-source approaches. Regional applications of EB approaches are enabled when the impact of errors in the LST and air temperature boundary conditions are reduced. [Anderson et al. \(2007\)](#) achieved this by basing the physical retrieval of the two-source EB approach on the rate of change in surface temperature during the morning. This reduces the impact of errors in the absolute (instantaneous) LST and air temperature retrievals and forms the basis of a multiscale integrated approach to estimating ET that is detailed in [Section 5.3.2](#).

### 5.3.1 GLEAM, a water balance approach to estimating evaporative stress

An example of a bottom-up approach to estimating evaporative stress is GLEAM: Global Land Evaporation, Amsterdam Methodology ([Miralles et al., 2011](#); [Martens et al., 2017](#)). It contains an observation-driven LSM specifically tailored to estimate global ET for long-term climatological

analysis (e.g., [Miralles et al., 2014](#)). The LSM consists of a multilayer running-water-balance to estimate root zone water. Inputs to the water-balance are observed precipitation, and soil moisture observations (from PMW sensors). Central to this methodology is the use of P-T formulations to model potential evaporation based on insolation and temperature inputs (see [Section 5.1](#)).

The actual evaporation and transpiration are calculated as a fraction of Ep using parameterizations of evaporative stress. The stress is partly based on the modeled water availability in the surface layers which accounts for past precipitation, evaporation, and drainage. Estimates of evaporative stress for vegetation further account for vegetation water content through PMW measurements of vegetation optical depth. GLEAM includes separate stress functions and  $\alpha$  for three dynamic surface components that contribute to ET: bare soil, short vegetation, tall vegetation.

GLEAM features the first global implementation of the Gash analytic model for the estimation of evaporation of intercepted rain water ([Gash, 1979](#); [Valente et al., 1997](#)). The volume of water that evaporates from the wet canopy during and immediately after a rain storm is estimated as a fraction of daily rainfall. The model parameters further account for canopy cover fraction, canopy storage, mean rainfall rates, and evaporation rates during wet canopy conditions ([Miralles et al., 2010](#)). A novel feature is the use of observed lightning frequency ([Cecil et al., 2014](#)) to distinguish synoptic from convective precipitation to account for the associated differences in rain rates.

Snow depth estimates from PMW observations are used to divert precipitation into a snowpack that is subject to sublimation before the eventual melt and entry into the soil water reservoir. The contribution of lakes and rivers is not modeled so that the total evaporation estimated by GLEAM only refers to the land fraction of the total surface area.

GLEAM is designed to be implemented for the entire duration of the modern satellite record and has been used to create daily ET records at 0.25-degree resolution from 1980 to present. These long-term ET records have been used in a series of recent hydrological and climate studies to study the impact of climate change and El Nino Southern oscillations on the water cycle, land-atmosphere feedbacks, hydrometeorological extremes, benchmarking and evaluating climate models ([Zhang et al., 2016](#); [Miralles et al., 2014](#)).

### 5.3.2 ALEXI: an integrated framework for two-source EB estimates of evaporation

The Atmosphere–Land Exchange Inverse (ALEXI) model ([Anderson et al., 2007](#); [Mecikalski et al., 1999](#)) combines two-source energy balance models ([Kustas and Norman, 1999](#); [Norman et al., 1995](#)) with atmospheric boundary layer (ABL) formulations for regional ET estimation. Model outputs include total ET, and estimates of soil evaporation and transpiration separately, with partitioning guided in part by the local vegetation cover fraction. ALEXI enables regional application of the two-source EB by basing the physical retrieval on the rate of change in surface temperature during the morning, reducing the impact of errors in the absolute (instantaneous) LST retrievals and in the air temperature boundary conditions.

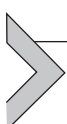
The available energy is based on top-of-atmosphere shortwave and longwave radiances, albedo estimates, and longwave radiation calculated from LST according to Stefan–Boltzman’s law. Ground heat flux is estimated as a fixed percent of net radiation. LAI is used for partitioning incoming radiation ([Anderson et al., 2007](#)). A set of equations describes the energy balance for soil to atmosphere fluxes and vegetation to atmosphere.

The ABL model simulates the changes in air temperature between the time of the morning LST observation (ideally 1 hour after sunrise) and the midday observation (ideally 1 hour before solar noon). The ABL-modeled air temperature at a reference height above the canopy provides a boundary condition that is consistent with the surface fluxes generated by the EB model. P-T Ep serves as an initial estimate for canopy evaporation and is iteratively reduced until the closed energy balance produces soil evaporation that is nonnegative. This procedure is based on the assumption that no condensation occurs during clear-sky daytime hours ([Kustas and Norman, 1999, 2000](#)).

Although ALEXI was developed for geostationary sensors ([Anderson et al., 2007](#)), global implementations with MODIS-LST ([Hain and Anderson, 2017](#); [Holmes et al., 2018](#)) are now routinely available through NASA’s Short-term Prediction Research and Transition (SPoRT). Combined with a long-term climatological record, the ratio of ALEXI ET over Ep is also used as an evaporative stress index to diagnose and monitor agricultural drought conditions ([Anderson et al., 2011a](#)). Because an EB-model like ALEXI does not model water availability it can be used

to identify neglected sources and sinks of water in LSM's, such as ground-water depth, irrigation extent, and tile drainage density (Yilmaz et al., 2014; Hain et al., 2015).

Importantly, ALEXI is part of an integrated framework of multiscale ET estimation (Anderson et al., 2011b) that also includes a flux disaggregation scheme (disALEXI: Norman et al., 2003; Anderson et al., 2004). DisALEXI utilizes higher resolution LST measurements (e.g., Landsat, or airborne platforms) to disaggregate the continental scale physical ALEXI retrievals of daily ET. On the days with high-resolution thermal observations this approach compares well with eddy-covariance measurements from flux towers. In a final step to the multiscale ET analysis framework, the Spatial and Temporal Adaptive Reflectance Fusion Model (STARFM) (Gao et al., 2006) is applied to generate a time-continuous, daily ET product at the fine spatial resolution of the disALEXI output. This ET fusion approach has been successfully demonstrated over rain-fed and irrigated cotton, corn, and soybean fields (Cammalleri et al., 2014; Yang et al., 2017), irrigated vineyards (Semmens et al., 2016), as well as forested landscapes (Yang et al., 2017).



## 5.4 New developments

Intermodel comparisons of global evaporation products show that they are able to capture important aspects of seasonality and spatial distribution related to climate regimes (Jimenez et al., 2011; Mueller et al., 2013; Michel et al., 2016; Miralles et al., 2016). However, these studies also reveal a lack of agreement between models in terms of the relative contribution of soil evaporation, plant transpiration, and evaporation of the intercepted water to the total evaporation at a global scale. This reflects the large uncertainties of the contribution of transpiration (Wei et al., 2017), but also the treatment of interception as a distinct process. In general, current LSMs are found to underestimate the transpiration contribution to global E compared to estimates from in situ data, satellite products, and isotope measurements (Schlesinger and Jasechko, 2014). These disagreements in the ratio of T to total ET are a significant contributor to uncertainty in long-term predictions of changes in the coupled carbon and water cycle. New measurements that can be used to better estimate

photosynthetic activity (Frankenberg et al., 2011), and thus water loss through transpiration, may allow for better observational constraints on the evaporation estimation.

Although surface energy balance approaches have a long legacy, long consistent records of global-scale ET estimates based on EB approach were not available until recently. This explains the lack of representation of EB approaches in the global evaporation comparisons discussed above, with SEBS as the lone exception. As was shown in Section 5.3.2, this situation is now changing and future assessments of global evaporation may be able to draw upon the full range of evaporation estimation approaches. Another development that will enhance the utility for EB approaches to climate science is in the application of more cloud-tolerant microwave observations to the estimation of LST (Holmes et al., 2009, 2016). This is intended to solve a central limitation of TIR-based LST, that no surface information penetrates clouds in the TIR frequency bands. This effectively limits (and biases) the temporal sampling of TIR-based approaches to clear conditions. The utility of microwave-based LST for EB estimates of evaporation has been demonstrated in the context of the ALEXI framework (Holmes et al., 2018). A full integration of PMW LST into the ALEXI framework will reduce the need for interpolation between days with clear-sky conditions and reduce uncertainty related to cloud filtering efficacy.

## References

- Allen, R.G., Pereira, L.S., Raes, D., Smith, M., 1998. Crop evapotranspiration—Guidelines for computing crop water requirements—FAO Irrigation and drainage paper 56. FAO, Rome, 300 (9), D05109.
- Allen, R.G., Pereira, L.S., Howell, T.A., Jensen, M.E., 2011. Evapotranspiration information reporting: I. Factors governing measurement accuracy. *Agric. Water Manage.* 98 (6), 899–920.
- Allen, R.G., Tasumi, M., Trezza, R., 2007. Satellite-based energy balance for mapping evapotranspiration with internalized calibration (METRIC)—model. *J. Irrig. Drain. Eng.* 133 (4), 380–394.
- Anderson, M.C., Norman, J.M., Mecikalski, J.R., Torn, R.D., Kustas, W.P., Basara, J.B., 2004. A multiscale remote sensing model for disaggregating regional fluxes to micrometeorological scales. *J. Hydrometeorol.* 5 (2), 343–363.
- Anderson, M.C., Norman, J.M., Mecikalski, J.R., Otkin, J.A., Kustas, W.P., 2007. A climatological study of evapotranspiration and moisture stress across the continental United States based on thermal remote sensing: 2. Surface moisture climatology. *J. Geophys. Res. Atmosph.* 112 (D11).
- Anderson, M.C., Norman, J.M., Kustas, W.P., Houborg, R., Starks, P.J., Agam, N., 2008. A thermal-based remote sensing technique for routine mapping of land-surface carbon, water and energy fluxes from field to regional scales. *Remote Sens. Environ.* 112 (12), 4227–4241.

- Anderson, M.C., Hain, C., Wardlow, B., Pimstein, A., Mecikalski, J.R., Kustas, W.P., 2011a. Evaluation of drought indices based on thermal remote sensing of evapotranspiration over the continental United States. *J. Climate* 24 (8), 2025–2044.
- Anderson, M.C., Kustas, W.P., Norman, J.M., Hain, C.R., Mecikalski, J.R., Schultz, L., et al., 2011b. Mapping daily evapotranspiration at field to continental scales using geostationary and polar orbiting satellite imagery. *Hydrol. Earth Syst. Sci.* 15 (1), 223–239.
- Baldocchi, D., Falge, E., Gu, L., Olson, R., Hollinger, D., Running, S., et al., 2001. FLUXNET: a new tool to study the temporal and spatial variability of ecosystem-scale carbon dioxide, water vapor, and energy flux densities. *Bull. Am. Meteorol. Soc.* 82 (11), 2415–2434.
- Bastiaanssen, W.G., Menenti, M., Feddes, R.A., Holtslag, A.A.M., 1998. A remote sensing surface energy balance algorithm for land (SEBAL). 1. Formulation. *J. Hydrol.* 212, 198–212.
- Cammalleri, C., Anderson, M.C., Gao, F., Hain, C.R., Kustas, W.P., 2014. Mapping daily evapotranspiration at field scales over rainfed and irrigated agricultural areas using remote sensing data fusion. *Agric. Forest Meteorol.* 186, 1–11.
- Carlson, T.N., Ripley, D.A., 1997. On the relation between NDVI, fractional vegetation cover, and leaf area index. *Remote Sensing Environ.* 62 (3), 241–252.
- Cavero, J., Medina, E.T., Puig, M., Martínez-Cob, A., 2009. Sprinkler irrigation changes maize canopy microclimate and crop water status, transpiration, and temperature. *Agron. J.* 101 (4), 854–864.
- Cecil, D.J., Buechler, D.E., Blakeslee, R.J., 2014. Gridded lightning climatology from TRMM-LIS and OTD: dataset description. *Atmosph. Res.* 135, 404–414.
- Cleugh, H.A., Leuning, R., Mu, Q., Running, S.W., 2007. Regional evaporation estimates from flux tower and MODIS satellite data. *Remote Sens. Environ.* 106 (3), 285–304.
- Dorigo, W., Wagner, W., Albergel, C., Albrecht, F., Balsamo, G., Brocca, L., et al., 2017. ESA CCI Soil Moisture for improved Earth system understanding: state-of-the art and future directions. *Remote Sensing Environ.* 203, 185–215.
- Fisher, J.B., Tu, K.P., Baldocchi, D.D., 2008. Global estimates of the land–atmosphere water flux based on monthly AVHRR and ISLSCP-II data, validated at 16 FLUXNET sites. *Remote Sens. Environ.* 112 (3), 901–919.
- Frankenberg, C., Fisher, J.B., Worden, J., Badgley, G., Saatchi, S.S., Lee, J.E., et al., 2011. New global observations of the terrestrial carbon cycle from GOSAT: Patterns of plant fluorescence with gross primary productivity. *Geophys. Res. Lett.* 38 (17).
- Gao, F., Masek, J., Schwaller, M., Hall, F., 2006. On the blending of the Landsat and MODIS surface reflectance: predicting daily Landsat surface reflectance. *IEEE Trans. Geosci. Remote sens.* 44 (8), 2207–2218.
- Gash, J.H.C., 1979. An analytical model of rainfall interception by forests. *Q J Roy Meteor. Soc.* 105 (443), 43–55.
- Hain, C.R., Anderson, M.C., 2017. Estimating morning change in land surface temperature from MODIS day/night observations: Applications for surface energy balance modeling. *Geophys. Res. Lett.* 44 (19), 9723–9733.
- Hain, C.R., Crow, W.T., Anderson, M.C., Yilmaz, M.T., 2015. Diagnosing neglected soil moisture source–sink processes via a thermal infrared–based two-source energy balance model. *J. Hydrometeorol.* 16 (3), 1070–1086.
- Holmes, T.R.H., De Jeu, R.A.M., Owe, M., Dolman, A.J., 2009. Land surface temperature from Ka band (37 GHz) passive microwave observations. *J. Geophys. Res. Atmosph.* 114 (D4).

- Holmes, T.R., Hain, C.R., Anderson, M.C., Crow, W.T., 2016. Cloud tolerance of remote-sensing technologies to measure land surface temperature. *Hydrol. Earth Syst. Sci.* 20 (8), 3263.
- Holmes, T.R.H., Hain, C.R., Crow, W.T., Anderson, M.C., Kustas, W.P., 2018. Microwave implementation of two-source energy balance approach for estimating evapotranspiration. *Hydrol. Earth Syst. Sci.* 22 (2), 1351.
- Jackson, D.L., Wick, G.A., Robertson, F.R., 2009. Improved multisensor approach to satellite-retrieved near-surface specific humidity observations. *J. Geophys. Res. Atmosph.* 114 (D16).
- Jasechko, S., Sharp, Z.D., Gibson, J.J., Birks, S.J., Yi, Y., Fawcett, P.J., 2013. Terrestrial water fluxes dominated by transpiration. *Nature* 49 (7445), 347.
- Jimenez, C., Prigent, C., Mueller, B., Seneviratne, S.I., McCabe, M.F., Wood, E.F., et al., 2011. Global intercomparison of 12 land surface heat flux estimates. *J. Geophys. Res. Atmosph.* 116 (D2).
- Jung, M., Reichstein, M., Ciais, P., Seneviratne, S.I., Sheffield, J., Goulden, M.L., et al., 2010. Recent decline in the global land evapotranspiration trend due to limited moisture supply. *Nature* 467 (7318), 951.
- Konings, A.G., Gentine, P., 2017. Global variations in ecosystem-scale isohydricity. *Global Change Biol.* 23 (2), 891–905.
- Konings, A.G., Williams, A.P., Gentine, P., 2017. Sensitivity of grassland productivity to aridity controlled by stomatal and xylem regulation. *Nat. Geosci.* 10 (4), 284.
- Kustas, W.P., Norman, J.M., 1999. Evaluation of soil and vegetation heat flux predictions using a simple two-source model with radiometric temperatures for partial canopy cover. *Agric. Forest Meteorol.* 94 (1), 13–29.
- Kustas, W.P., Norman, J.M., 2000. A two-source energy balance approach using directional radiometric temperature observations for sparse canopy covered surfaces. *Agron. J.* 92 (5), 847–854.
- Liu, Y.Y., Dijk, A.I., McCabe, M.F., Evans, J.P., Jeu, R.A., 2013. Global vegetation biomass change (1988–2008) and attribution to environmental and human drivers. *Global Ecol. Biogeogr.* 22 (6), 692–705.
- Martens, B., Gonzalez Miralles, D., Lievens, H., Van Der Schalie, R., De Jeu, R.A.M., Fernández-Prieto, D., et al., 2017. GLEAMv3: Satellite-based land evaporation and root-zone soil moisture. *Geosci. Model Dev.* 10 (5), 1903–1925.
- Mecikalski, J.R., Diak, G.R., Anderson, M.C., Norman, J.M., 1999. Estimating fluxes on continental scales using remotely sensed data in an atmospheric-land exchange model. *J Appl. Meteorol.* 38 (9), 1352–1369.
- Michel, D., Jiménez, C., Miralles, D.G., Jung, M., Hirschi, M., Ershadi, A., et al., 2016. The WACMOS-ET project – part 1: tower-scale evaluation of four remote-sensing-based evapotranspiration algorithms. *Hydrol. Earth Syst. Sci.* 20 (2), 803–822. Available from: <https://doi.org/10.5194/hess-20-803-2016>.
- Miralles, D.G., Gash, J.H., Holmes, T.R.H., de Jeu, R.A.M., Dolman, A.J., 2010. Global canopy interception from satellite observations. *J. Geophys. Res.* 115 (D16), D16122. Available from: <https://doi.org/10.1029/2009JD013530>.
- Miralles, D.G., De Jeu, R.A.M., Gash, J.H., Holmes, T.R.H., Dolman, A.J., 2011. An application of GLEAM to estimating global evaporation. *Hydrol. Earth Syst. Sci. Discuss.* 8 (1).
- Miralles, D.G., Van Den Berg, M.J., Gash, J.H., Parinussa, R.M., De Jeu, R.A.M., Beck, H.E., et al., 2014. El Niño–La Niña cycle and recent trends in continental evaporation. *Nat. Clim. Change* 4 (2), 122.
- Miralles, D.G., Jiménez, C., Jung, M., Michel, D., Ershadi, A., McCabe, M.F., et al., 2016. The WACMOS-ET project, part 2: evaluation of global terrestrial evaporation data sets. *Hydrol. Earth Syst. Sci.* 20 (2), 823–842.

- Momen, M., Wood, J.D., Novick, K.A., Pangle, R., Pockman, W.T., McDowell, N.G., et al., 2017. Interacting effects of leaf water potential and biomass on vegetation optical depth. *J. Geophys. Res. Biogeosci.* 122 (11), 3031–3046.
- Monteith, J.L., 1965. Evaporation and environment. *Symp. Soc. Exp. Biol.* 19 (205–23), 4.
- Mu, Q., Zhao, M., Running, S.W., 2011. Improvements to a MODIS global terrestrial evapotranspiration algorithm. *Remote Sens. Environ.* 115 (8), 1781–1800.
- Mueller, B., Hirschi, M., Jimenez, C., Ciais, P., Dirmeyer, P.A., Dolman, A.J., et al., 2013. Benchmark products for land evapotranspiration: LandFlux-EVAL multi-data set synthesis. *Hydrol. Earth Syst. Sci.* Available from: <http://repository.kaust.edu.sa/kaust/handle/10754/334520>.
- Mueller, N.D., Butler, E.E., McKinnon, K.A., Rhines, A., Tingley, M., Holbrook, N.M., Huybers, P., 2016. Cooling of US Midwest summer temperature extremes from cropland intensification. *Nat. Clim. Change* 6 (3), 317.
- Norman, J.M., Kustas, W.P., Humes, K.S., 1995. Source approach for estimating soil and vegetation energy fluxes in observations of directional radiometric surface temperature. *Agric. For. Meteorol.* 77 (3–4), 263–293. Available from: [https://doi.org/10.1016/0168-1923\(95\)02265-Y](https://doi.org/10.1016/0168-1923(95)02265-Y).
- Norman, J.M., Anderson, M.C., Kustas, W.P., French, A.N., Mecikalski, J., Torn, R., et al., 2003. Remote sensing of surface energy fluxes at 101-m pixel resolutions. *Water Resour. Res.* 39 (8), 1221.
- Oki, T., Kanae, S., 2006. Global hydrological cycles and world water resources. *Science* 313 (5790), 1068–1072.
- Otkin, J.A., Anderson, M.C., Hain, C., Svoboda, M., Johnson, D., Mueller, R., et al., 2016. Assessing the evolution of soil moisture and vegetation conditions during the 2012 United States flash drought. *Agric. Forest Meteorol.* 218, 230–242.
- Owe, M., de Jeu, R., Holmes, T., 2008. Multisensor historical climatology of satellite-derived global land surface moisture. *J. Geophys. Res. Earth Surface* 113 (F1).
- Prigent, C., Jimenez, C., Aires, F., 2016. Toward “all weather,” long record, and real-time land surface temperature retrievals from microwave satellite observations. *J. Geophys. Res. Atmosph.* 121 (10), 5699–5717.
- Priestley, C.H.B., Taylor, R.J., 1972. On the assessment of surface heat flux and evaporation using large-scale parameters. *Mon. Weather Rev.* 100 (2), 81–92.
- Schlesinger, W.H., Jasechko, S., 2014. Transpiration in the global water cycle. *Agr. Forest Meteorol.* 189, 115–117.
- Seemanns, K.A., Anderson, M.C., Kustas, W.P., Gao, F., Alfieri, J.G., McKee, L., et al., 2016. Monitoring daily evapotranspiration over two California vineyards using Landsat 8 in a multi-sensor data fusion approach. *Remote Sens. Environ.* 185, 155–170.
- Senay, G.B., Friedrichs, M.K., Singh, R.K., Velpuri, N.M., 2016. Evaluating landsat 8 evapotranspiration for water use mapping in the Colorado river basin. *Remote Sens. Environ.* 185, 171–185.
- Serbin, S.P., Singh, A., McNeil, B.E., Kingdon, C.C., Townsend, P.A., 2014. Spectroscopic determination of leaf morphological and biochemical traits for northern temperate and boreal tree species. *Ecol. Appl.* 24 (7), 1651–1669.
- Skofronick-Jackson, G., Petersen, W.A., Berg, W., Kidd, C., Stocker, E.F., Kirschbaum, D.B., et al., 2017. The global precipitation measurement (GPM) mission for science and society. *Bull. Am. Meteorol. Soc.* 98 (8), 1679–1695.
- Smith, E.A., Asrar, G., Furuhama, Y., Ginatti, A., Mugnai, A., Nakamura, K., et al., 2007. International global precipitation measurement (GPM) program and mission: an overview. In *Measuring Precipitation From Space*. Springer, Dordrecht, pp. 611–653.
- Su, Z., 2002. The Surface Energy Balance System (SEBS) for estimation of turbulent heat fluxes. *Hydrol. Earth Syst. Sci.* 6 (1), 85–100.

- Tomita, H., Hihara, T., Kubota, M., 2018. Improved satellite estimation of near-surface humidity using vertical water vapor profile information. *Geophys. Res. Lett.* 45 (2), 899–906.
- Valente, F., David, J.S., Gash, J.H.C., 1997. Modelling interception loss for two sparse eucalypt and pine forests in central portugal using reformulated rutter and gash analytical models. *J. Hydrol.* 190 (1–2), 141–162.
- Wei, Z., Yoshimura, K., Wang, L., Miralles, D.G., Jasechko, S., Lee, X., 2017. Revisiting the contribution of transpiration to global terrestrial evapotranspiration. *Geophys. Res. Lett.* 44 (6), 2792–2801.
- Wolfe, G.M., Kawa, S.R., Hanisco, T.F., Hannun, R.A., Newman, P.A., Swanson, A., et al., 2018. The NASA Carbon Airborne Flux Experiment (CARAFE): instrumentation and methodology. *Atmosph. Measurement Tech.* 11 (3), 1757.
- Yang, Y., Anderson, M.C., Gao, F., Hain, C.R., Semmens, K.A., Kustas, W.P., et al., 2017. Daily landsat-scale evapotranspiration estimation over a forested landscape in North Carolina, USA, using multi-satellite data fusion. *Hydrol. Earth Syst. Sci.* 21 (2), 1017–1037.
- Yilmaz, M.T., Anderson, M.C., Zaitchik, B., Hain, C.R., Crow, W.T., Ozdogan, M., et al., 2014. Comparison of prognostic and diagnostic surface flux modeling approaches over the Nile River basin. *Water Resour. Res.* 50 (1), 386–408.
- Zhang, Y., Peña-Arancibia, J.L., McVicar, T.R., Chiew, F.H.S., Vaze, J., Liu, C., et al., 2016. Multi-decadal trends in global terrestrial evapotranspiration and its components. *Sci. rep.* 6, 19124.